Journal of Research in Applied and Basic Medical Sciences 2023; 9(3): 143-153

Original Article

RABMS Journal of Research in Applied and Basic Medical Sciences

Analysis the Effectiveness of Remdesivir, Galidesivir, Sofosbuvir, Tenofovir and Ribavirin as Potential Therapeutic Drug target against SARS-Cov-2 RNA-Dependent RNA Polymerase (RdRp): An *in Silico* Docking Study

Rajneesh Prajapat [1*], Suman Jain [2]

[1] *Ph.D Department of Biochemistry, Pacific Institute of Medical Sciences, Sai Tirupati University, Udaipur, Rajasthan, India*

[2] *Ph.D Department of Biochemistry, Pacific Institute of Medical Sciences, Sai Tirupati University, Udaipur, Rajasthan, India*

***Corresponding author:** *Rajneesh Prajapat,* **Address**: Department of Biochemistry, Pacific Institute of Medical Sciences, Sai Tirupati University, Udaipur, Rajasthan, India, **Email**: *rajneesh030041@gmail.com,* **Tel**: *+91-7976055027*

Abstract

***Background & Aims*:** The active site of RdRp-CoV is highly conserved, with two successive and surface-accessible aspartates in a beta-turn structure. Antiviral drugs Remdesivir, Galidesivir, Tenofovir, Sofosbuvir, and Ribavirin are known as inhibitors of RdRps, while lopinavir and rotinavir are known inhibitors of main protease (MPro) of coronavirus. The aim of the present study was to *in silico* test of the effectiveness of anti-polymerase drugs against SARS-CoV-2 RdRp, including 5 FDA-approved antiviral medications.

***Materials & Methods*:** RdRp-CoV (nsp12) plays an important role in virus replication; therefore, it serves as a target to development of antiviral drugs. In this study, the RdRp is modeled, validated, and then targeted using different anti-polymerase drugs that approved for use against various viruses.

***Results*:** The five approved drugs (Galidesivir, Remdesivir, Tenofovir, Sofosbuvir, and Ribavirin) were able to bind the SARS-CoV-2 RdRp with binding energies of 42.6, 1.7, 38.4, -1.4, and -3.9 kcal/mol, respectively. For the drug ribavirin, the only interactions established upon docking were the 11 H-bonds with F165, N459, R624, P677, N791, L460, N791, T462, N628, and T462 of the SARS-CoV-2 RdRp.

***Conclusion*:** The results suggest the effectiveness of Ribavirin, Remdesivir, Sofosbuvir, Galidesivir, and Tenofovir as potent drugs against RdRp-CoV since they tightly bind to RdRp. The availability of FDA-approved anti-RdRp drugs can help treat the infection of new variant of SARS-CoV-2 strain specifically.

***Keywords*:** Antiviral drugs, FDA, in silico, Remdesivir, RdRp, SARS-CoV-2

Received 07 February 2023; accepted for publication 28 May 2023

Introduction

In December 2019, a rapid outbreak of a novel coronavirus designated as COVID-19, reported from the city of Wuhan, China (1–2). On January 30, 2020, World Health Organization (WHO) declared that the outbreak of novel coronavirus (2019-nCoV) constitutes a Public Health Emergency of International Concern (PHEIC) (3-4). The current pandemic caused by the nCoV-2019 has reached nearly all the countries of the world (5), and on WHO dashboard, 664,618,938 confirmed cases of COVID-19 with more than 6,722,949 deaths reported till 24 January 2023. The two strains of SARS have been identified that cause epidemics: (1) SARS-CoV, identified in 2002–2004, and (2) novel coronavirus (SARS-CoV-2), that emerged as a potential threat in late 2019 (6). The symptoms of COVID-19 include fever, malaise, dry cough, shortness of breath, and respiratory distress (7-8).

Severe Acute Respiratory Syndrome Coronavirus (SARS-CoV) is a positive-sense single-stranded RNA (30,000 bp) virus from the genus *Betacoronavirus*, commonly known to infect bats, humans, and other mammals (9-10).

Genome of SARS-CoV contains 5′ and 3′ untranslated regions (UTR's) for characteristic genes coding for spike (S) marking all coronaviruses, nucleocapsid (N), matrix (M), and envelope (E), and non-structural proteins, such as proteases (nsp3 and nsp5) and RdRp (nsp12) (11-13). RdRP (nsp12) plays an important role in virus replication by serving as the target site for antiviral drugs (14). RdRp is a conserved enzymatic protein within RNA viruses, and thus could be used as a target to development of antiviral drugs (15-16). The active site of RdRp is highly conserved with two successive and surface-accessible aspartates in a beta-turn structure (17-19).

Antiviral drugs remdesivir, galidesivir, tenofovir, sofosbuvir, and ribavirin are known inhibitors of RdRps (20-21), while lopinavir and rotinavir are known inhibitors of main protease (MPro) of coronavirus (22-23).

Presently, there is no effective and specific drug available for the treatment of COVID-19, except remdesivir and favipiravir which are successful up to some extent. In this study, the SARS-CoV-2 RdRp model was built using the SARS RdRp solved structures from the NCBI and protein data bank (PDB) (24).

The homology modeling and docking was performed to test the effectiveness of anti-polymerase drugs against SARS-CoV-2 RdRp, including 5 FDA-approved medications used for the treatment of HCV, HIV, and the Ebola virus (25-26).

The results were implied that the currently available treatments may be able to effectively suppress the newly emerged coronavirus (27).

Materials & Methods

Sequence alignment and homology modeling:

The RNA-dependent RNA polymerase (RdRp) sequence of SARS-CoV-2 (YP_009725307) was retrieved from the NCBI database (28). A homology model for the SARS-CoV-2 RdRp was built using the Swiss Model web server (29). The SARS-CoV-2 RdRp (PDB ID: 7UO9) was employed as a template for building homology model since it was the most sequelogous solved structure (97.08% sequence identity) to SARS-CoV-2 RdRp. 7UO9 is a SARS-CoV-2 replication-transcription complex bound to UTP (cryo-electron microscopy) with 3.13 Å resolution.

The Structure Analysis and Verification Server (SAVES) server was used to examine the model (30). Various types of software were used for validation of the model e.g., PROCHECK (31), Verify 3D (32), and ERRAT (33), in addition to the Ramachandran plot of the MolProbity web server. MolProbity is a widely used system of model validation for protein and nucleic acid structures (34-35). Model minimization was performed after the addition of missed hydrogen atoms to prepare for the docking study (41). ProSA server was used to determine the potential errors in the 3D model (36).

Molecular Docking:

SeamDock software (https://bioserv.rpbs.univ-paris-diderot.fr/) was utilized in all the docking experiments, with the optimized SARS-CoV-2 RdRp model as the docking target (37). In addition, SARS-CoV-2 replication-transcription complex (PDB ID: 7uo9) was used as docking targets for comparison. A total of 5 compounds were tested against SARS-CoV-2 RdRp (YP_009725307) and its homologous RdRp (7UO9), five approved drugs against different viral RdRps (Galidesivir, Remdesivir, Tenofovir, Sofosbuvir, and Ribavirin). All the compounds were prepared to be optimized in their active forms in physiological conditions.

Results

SARS-CoV-2 RdRp Modeling:

The SARS-CoV-2 RdRp model (932 residues) was generated by homology modeling using the Swiss Model web server. The SARS-CoV-2 replication-transcription complex (PDB ID: 7UO9) was employed as a template.

The Swiss model created a high-quality model based on the sequence identity between the SARS-CoV-2 RdRp and 7UO9.

Protein Model Building:

The sequence alignment between the target and template was performed using BLASTp against PDB database (38). The 3D ribbon model of SARS-CoV-2 RdRp (YP_009725307) generated using SWISS-MODEL (https://swissmodel.expasy.org) structure assessment tool (Figure 1).

Fig. 1. The 3D ribbon structure model of SARS-CoV-2 RdRp (YP_009725307)

Model Reputation:

The SARS-CoV-2 RdRp (YP_009725307) model corresponding to probability confirmation with 89.2% residue of the core section, 10.4% of the allowed section, and 0.4 % residue of the outer section in the Ramachandran plot (39) (Figure 2a, b). The above results indicated the reliability of protein models (Table 1) (35, 36).

The model exhibited a very high (97.08%) sequence identity to the template, suggesting that an excellent model was obtained. Testing of the model validity was mediated by the Ramachandran plot (89.2 % in the core region), Verify-3D (89.52% of the residues have averaged 3D-1D score >= 0.2), and ERRAT (overall quality factor of 91.38 %) (Table 1).

Table 1. Evaluation of the protein model by PROCHECK, VERIFY-3D, and ERRAT

Template	PROCHECK				Verify-3D	ERRAT
	Core	Allowed	Generously outer	Disallowed	3D-ID Score	Overall Quality Factor
RdRp (YP_009725307)	89.2%	10.4%	0.4 %	0.1 %	89.52	91.38
7uo9	87.6%	12.2%	0.2%	0.0%	78.18	90.63

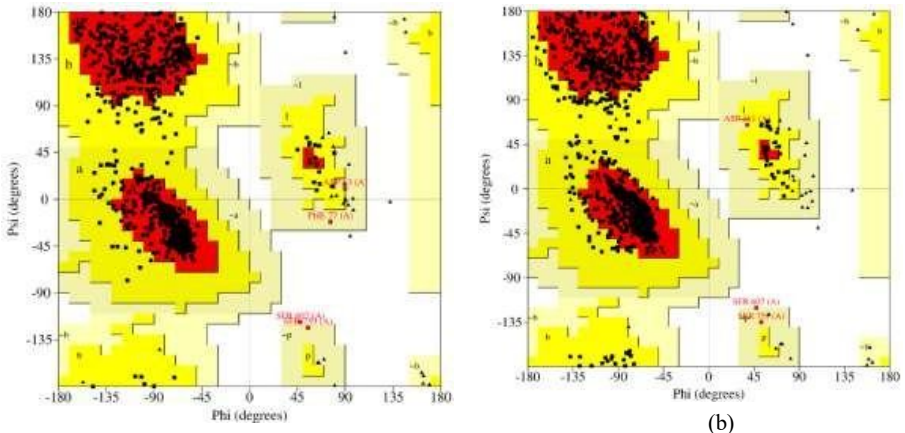

(a) (b)

Fig. 2. The Ramachandran plot of SARS-CoV-2 RdRp (YP_009725307) - (a) The total number of residues was 89.2% in the core, 10.4% in the allowed, and 0.4 % in the generously allowed regions; (b) Ramachandran plot of SARS-CoV-2 replication-transcription complex (7UO9) – The total number of residues was 87.6% in the core, 12.2% in the allowed, and 0.2 % in the generously allowed regions.

The verify-3D illustrates the compatibility of an atomic model (3D) with its amino acid sequence (1D) by assigning a structural class based on its location and environment (alpha, beta, loop, polar, and nonpolar) (Table 1) (40).

ERRAT analyses the statistics of non-bonded interactions between different atom types and plots the value of the error function versus position, which is calculated by comparison with statistics from highly refined structures (41). ERRAT overall quality factor of the model was 91.3813, with an average probability value of 5.05729 (Figure 3).

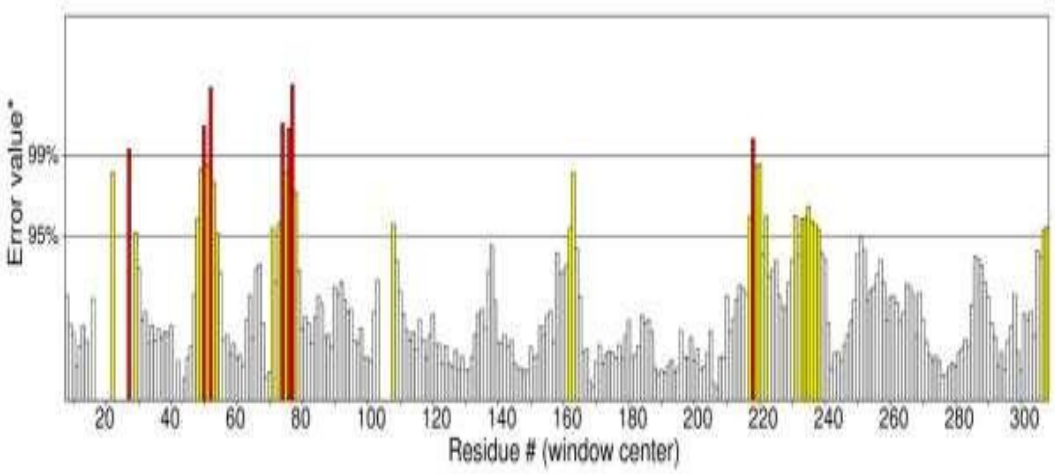

Fig. 3. ERRAT result showing an overall quality factor of 91.3813 for the model (error-axis showing the error values to reject regions that exceed the error value).

The individual components of MolProbity results including Clash score, Rotalyze, c-beta dev, bad contact, and angles are also separately available through the Phenix command line (Table 2). MolProbity allows selection of any combination of clashes, hydrogen bonds, and Van der Waals contacts to calculate and display on the structure (42).

Table 2. MolProbity results of SARS-CoV-2 RdRp (YP_009725307)

MolProbity parameters	Result	Residues
MolProbity Score	0.93	-
Clash Score	0.34	(A726 ARG-A729 GLU), (A291 ASP- A735 ARG)
Rotamer Outliers	0.24%	A790 ASN, A468 GLN
C-Beta Deviations	7	A161 ASP, A77 PHE, A63 ASP, A377 ASP, A362 HIS, A531 THR, A824 ASP
Bad Bonds	1 /7652	A790 ASN
Bad Angles	65 / 10385	-
Cis Prolines	1 / 30	(A504 PHE-A505 PRO)

The QMEANDisCo Global value of 0.89 ± 0.05 was observed for the SARS-CoV-2 RdRp (YP_009725307), which is very close to 0 and therefore an acceptable value (43). Assessed validity of the model predictable among 0 and 1, which could be concluded from the density plot locus set for QMEAN score (Figure 4). Figure 4 illustrates the QMEAN scores for the biological unit reference set, which were used as a tool for oligomeric protein assessment.

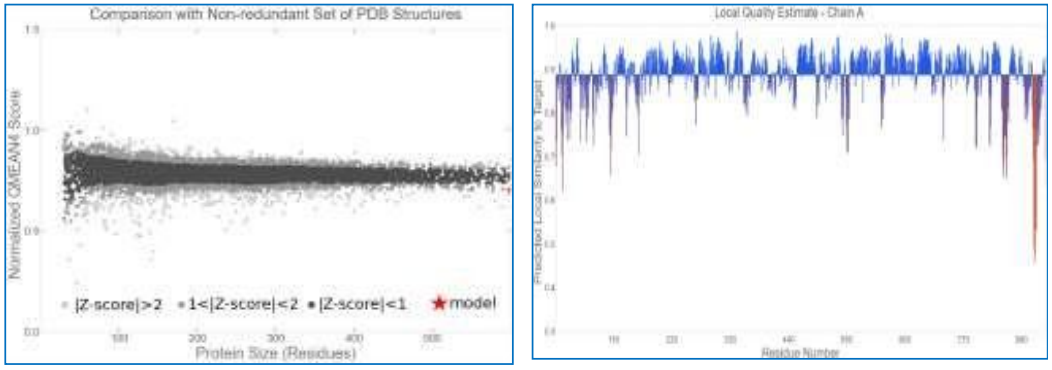

Fig. 4. QMEAN scores for a biological unit reference set of SARS-CoV-2 RdRp (YP_009725307). (a) Plot showing Z-score; (b) Local quality model for estimation of local summarily to target.

Validation of the Model:

ProSA was used to determine the potential errors in the 3D model of SARS-CoV-2 RdRp (YP_009725307) (44). The archived ProSA Z-score of -13 indicates two aspects: overall model quality and energy deviation (Figure 5).

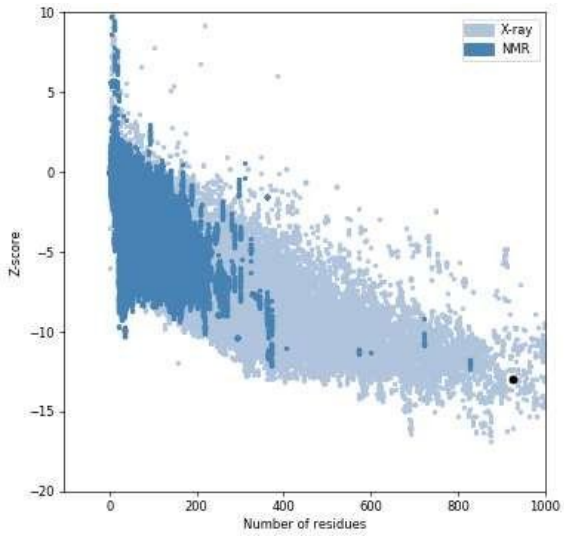

(a)

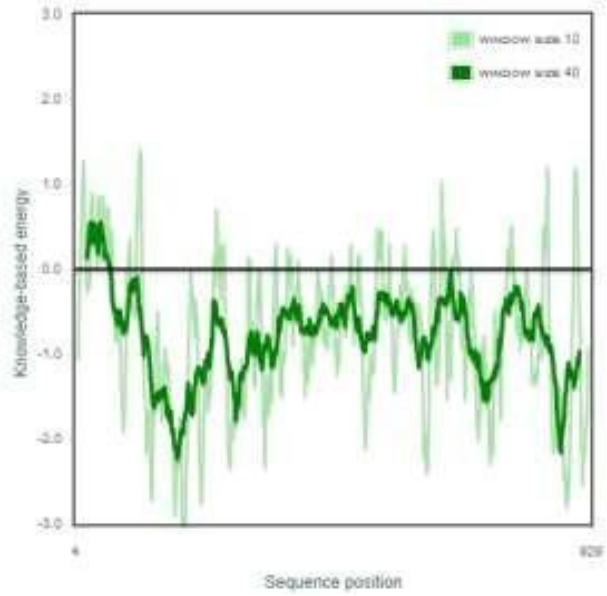

(b)

Fig. 5. ProSA examination of SARS-CoV-2 RdRp (YP_009725307) overall model quality. (a) The blue dot in the plot shows the -13 z-score of predicted models; (b) The residue score plot shows energies of amino acids are less than zero, which represents good local model quality.

Molecular Docking:

The binding pockets of SARS-CoV-2 RdRp (YP_009725307) are still not reported. Hence, the *in-silico* approaches were used for the prediction of binding pockets. The SeamDock docking server was used to explore the binding of ligands to the respective protein. The top five docking models of binding pockets of SARS-CoV-2 RdRp (YP_009725307) were identified and ranked based on the energy. More negative docking scores indicated higher binding affinity (Table 4). The

summary table contains two rows: the ranks and docking energy scores from the input structures. Model 1 has high accuracy with an interface docking score of 42.6 kcal/mol from the crystal structure (Table 3).

The binding pocket and interacting residues of the selected inhibitor Remdesivir was analyzed in 3D using SeamDock docking server (Figure 6).

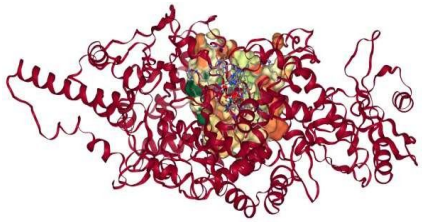

Fig. 6. Binding pocket and interacting residues of the analyzed inhibitor Remdesivir using SeamDock docking server.

The binding residues of the cavities were explored for the fruitful binding of novel ligands. The energy range of predicted cavities also indicated the efficacy of pockets. The mutational study of binding residues suggested that these residues could be used as a clinical prospectus for the effective treatment of COVID-19. The predicted binding residues lead to the drug designing of lead compounds against SARS-CoV-2 RdRp.

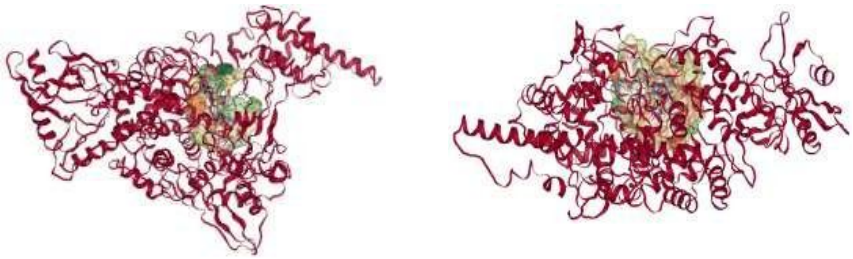

Fig. 7. Binding pocket and interacting residues of the analyzed inhibitor (a) Galidesivir, (b) Sofosbuvirusing SeamDock docking server

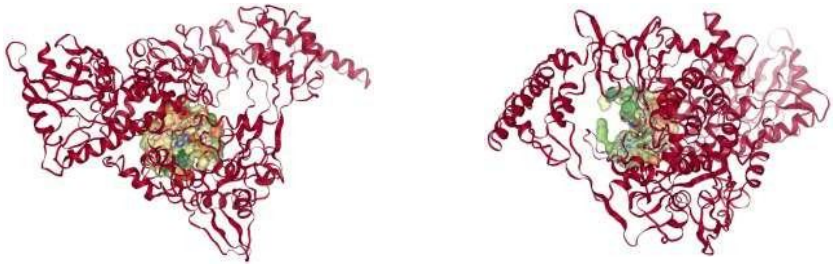

Fig. 8. Binding pocket and interacting residues of the analyzed inhibitor (a) Tenofovir, (b) Ribavirin using SeamDock docking server.

Table 3. Docking Results of receptor SARS-CoV-2 RdRp (YP_009725307) with ligand Remdesivir,Galidesivir, Sofosbuvir, Tenofovir and Ribavirin

SARS-CoV-2 RdRp (YP_009725307) Docking Interaction									
REMDESIVIR		**GALIDESIVIR**		**SOFOSBUVIR**		**TENOFOVIR**		**RIBAVIRIN**	
Hydrophobic Contact		**Ionic Interaction**		**Hydrophobic Contact**		**Hydrophobic Contact**		**Ionic Interaction**	
Ligand atom	Receptor	Ligand atom	Receptor	Ligand atom	Receptor	Ligand atom	Receptor	Ligand atom	Receptor
C23	V315(A) CB	N1	D760(A) OD1	C19	V315(A)CG1	C4	P461(A) CB	N1	D760(A) OD1
C27	V315(A) CG1	N5	D623(A) OD1	C9	Y458(A) CB			N4	D618(A) OD1
C26	E350(A) CG			C5	N459(A) CB				
C16	L460(A) CD2			C12	P461(A) CB				
C26	N628(A) CB			C9	A625(A) CB				
C22	P677(A) CB			C18	P627(A) CB				
C8	N791(A) CB			C15	N628(A) CB				
				C9	N791(A) CB				
				C9	V792(A)CG2				
Hydrogen Bond		**Hydrogen Bond**		**Hydrogen Bond**		**Hydrogen Bond**		**Hydrogen Bond**	
Ligand atom	Receptor	Ligand atom	Receptor	Ligand atom	Receptor	Ligand atom	Receptor	Ligand atom	Receptor
N6	F165(A) O	O2	P620(A) O	N3	N459(A) O	O4	N459(A) O	O5	D618(A) OD2
O6	N459(A) OD1	O1	D623(A) OD1	O2	T462(A) OG1	N2	L460(A) O	N3	Y619(A) O
N3	N459(A) OD1	N4	T680(A) OG1	N3	P677(A) O	N5	T462(A) O	O2	D623(A) OD1
O2	R624(A) O	N5	T687(A) OG1	O1	L460(A) N	N2	N628(A) N	O4	D760(A) OD1
O8	P677(A) O	N4	T680(A) OG1	O2	T462(A) OG1			O2	R555(A) NH1
N1	N791(A) O	N4	N691(A) ND2					O2	R555(A) NH2
O1	L460(A) N								
O1	N791(A) ND2								
O4	T462(A) OG1								
O6	N628(A) N								
O5	T462(A) N								
Weak Hydrogen Bond		**Weak Hydrogen Bond**		**Weak Hydrogen Bond**		**Weak Hydrogen Bond**		**Weak Hydrogen Bond**	
Ligand atom	Receptor	Ligand atom	Receptor	Ligand atom	Receptor	Ligand atom	Receptor	Ligand atom	Receptor
C2	Y458(A) O	C11	N691(A) OD1	C8	A625(A) O	C6	N459(A) OD1	C8	D618(A) OD2
C12	N459(A) OD1	N2	S682(A) CB	C3	N790(A) O	C6	L460(A) O	C5	D760(A) OD2
C18C6	N459(A) OD1	O1	K621(A) CA	C8	N790(A) O	C6	N628(A) OD1	C6	D760(A) OD2
C9	N459(A) OD1			C10	N791(A) O	C2	P677(A) O	C7	D760(A) OD2
C11	N791(A) O			O6	G678(A) CA	N2	P627(A) CA	O3	S682(A) CB
	N791(A) O					O3	P461(A) CD	O4	S759(A) CB
C13	N791(A) O								
O2	A625(A) CA								
O4	P627(A) CA								
O6	P627(A) CA								
O5	P461(A) CA								

Table 4. Docking affinity scores - kcal/mol

Docking Score - affinity (kcal/mol)				
Remdesivir	Galidesivir	Sofosbuvir	Tenofovir	Ribavirin
42.6	1.7	38.4	- 1.4	- 3.9

The binding pocket and interacting residues of the selected inhibitors were analyzed (Table 3; Figures 6 to 8).

Discussion

The five approved drugs (Galidesivir, Remdesivir, Tenofovir, Sofosbuvir, and Ribavirin) surrounded by the yellow-green globular structure (Figures 6 to 8), are able to bind the SARS-CoV-2 RdRp with binding energies of 42.6, 1.7, 38.4, -1.4, and -3.9 kcal/mol, respectively (Table 4).

These drugs were able to bind to the new coronavirus strain RdRp tightly, and hence may contradict the polymerase function. For the approved drug ribavirin, the interactions established upon docking were the 11 H-bonds with F165, N459, R624, P677, N791, L460, N791, T462, N628, and T462 of the SARS-CoV-2 RdRp. The same pattern was found for Galidesivir, but with a reduced number of H-bonds (6 H-bonds with P620, D623, T680, T687, T680, and N691, which was reflected in the binding energy values (42.6 and 1.7 kcal/mol for Ribavirin and Galidesivir, respectively). On the other hand, Sofosbuvir formed 5 H- bonds

(N459, T462, P677, L460, T462) and 09 hydrophobic contacts with the SARS-CoV-2 RdRp (Table 3).

The five approved drugs (Galidesivir, Remdesivir, Tenofovir, Sofosbuvir, and Ribavirin) could effectively interact to SARS-CoV-2 RdRp, with binding energies comparable to those of native nucleotides. The optimization of the compounds using the high-quality model of SARS-CoV-2 RdRp may result in develop perfect compound that able to control the newly emerged virus infection.

Conclusion

RdRp-CoV (nsp12) is serving as a potential target for the anti-polymerase drugs to inhibit virus replication. The results suggest the effectiveness of Ribavirin, Remdesivir, Sofosbuvir, Galidesivir, and Tenofovir as potent drugs against SARS-CoV-2 since they tightly bind to RdRp. The available FDA-approved anti-RdRp drugs that are currently in clinical trials or in the market could be used on the emergency basis for treatment of new viral infection COVID-19.

Acknowledgments

The authors are thankful to Dr. Indrajeet Singhvi (VC, Sai Tirupati University, Udaipur, Rajasthan, India) for his precious support and guidance during Ph.D coursework. The biochemistry and bioinformatics research group members are also acknowledged for technical support.

Ethical Statement

This study was approved by the Ethics Committee of Pacific Institute of Medical Sciences, Sai Tirupati University, Udaipur, Rajasthan, India (Ref. no: STU/IEC/2021/81).

Funding/Support

The authors did not receive any financial support for the research, and publication of this article.

Conflict of interest

The authors have no conflict of interest in this study.

References

1. Huang C, Wang Y, Li X, Ren L, Zhao J, Hu Y, Zhang L, Fan G, Xu J, Gu X, Cheng Z, Yu T, Xia J, Wei Y, Wu W, Xie X, Yin W, Li H, Liu M, Xiao Y, Gao H, Guo L, Xie J, Wang G, Jiang R, Gao Z, Jin Q, Wang J, Cao B. Clinical features of patients infected with 2019 novel coronavirus in Wuhan, China. Lancet 2020; 395(10223):497-506. doi: 10.1016/S0140-6736(20)30183-5.
2. Wu YC, Chen CS, Chan YJ. The outbreak of COVID-19: An overview. J Chin Med Assoc 2020;83 (3):217-20. doi: 10.1097/JCMA.0000000000000270.
3. Jee Y. WHO International Health Regulations Emergency Committee for the COVID-19 outbreak. Epidemiol Health 2020; 42:e2020013. doi: 10.4178/epih.e2020013.
4. Aftab SO, Ghouri MZ, Masood MU, Haider Z, Khan Z, Ahmad A, Munawar N. Analysis of SARS-CoV-2 RNA-dependent RNA polymerase as a potential therapeutic drug target using a computational approach. J Transl Med 2020;18(1):275. doi: 10.1186/s12967-020-02439-0.
5. Cucinotta D, Vanelli M. WHO Declares COVID-19 a Pandemic. Acta Biomed 2020;91(1):157-60. doi: 10.23750/abm.v91i1.9397.
6. Lau SK, Li KS, Huang Y, Shek CT, Tse H, Wang M, Choi GK, Xu H, Lam CS,Guo R, Chan KH. Ecoepidemiology and complete genome comparison of different strains of severe acute respiratory syndrome related Rhinolophus bat coronavirus in China reveals bats as a reservoir for acute, self-limiting infection that allows recombination events. J Virol 2010;84:2808-19.
7. Baj J, Karakuła-Juchnowicz H, Teresiński G, Buszewicz G, Ciesielka M, Sitarz R, Forma A, Karakuła K, Flieger W, Portincasa P, Maciejewski R. COVID-19: Specific and Non-Specific Clinical Manifestations and Symptoms: The Current State of Knowledge. J Clin Med 2020;9(6):1753. doi: 10.3390/jcm9061753.
8. Struyf T, Deeks JJ, Dinnes J, Takwoingi Y, Davenport C, Leeflang MM, Spijker R, Hooft L, Emperador D, Domen J, Tans A, Janssens S, Wickramasinghe D, Lannoy V, Horn SRA, Van den Bruel A; Cochrane COVID-19 Diagnostic Test Accuracy Group. Signs and symptoms to determine if a patient presenting in primary care or hospital outpatient settings has COVID-19. Cochrane Database Syst Rev 2022;5(5):CD013665. doi: 10.1002/14651858.CD013665.pub3.

9. Abdelrahman Z, Li M and Wang X. Comparative Review of SARS-CoV-2, SARS-CoV, MERS-CoV, and Influenza A Respiratory Viruses. Front Immunol 2020;11:552909. doi: 10.3389/fimmu.2020.552909.
10. Malik YA. Properties of Coronavirus and SARS-CoV-2. Malays J Pathol 2020;42(1):3-11.
11. Lai MM, Baric RS, Makino S, Keck JG, Egbert J, Leibowitz JL, Stohlman SA. Recombination between nonsegmented RNA genomes of murine coronaviruses. J Virol 1985;56:449-56.
12. Khailany RA, Safdar M, Ozaslan M. Genomic characterization of a novel SARS-CoV-2. Gene Rep 2020;19:100682. doi: 10.1016/j.genrep.2020.100682.
13. Naqvi AAT, Fatima K, Mohammad T, Fatima U, Singh IK, Singh A, Atif SM, Hariprasad G, Hasan GM, Hassan MI. Insights into SARS-CoV-2 genome, structure, evolution, pathogenesis and therapies: Structural genomics approach. Biochim Biophys Acta Mol Basis Dis 2020;1866(10):165878. doi: 10.1016/j.bbadis.2020.165878.
14. Woo PC, Huang Y, Lau SK, Tsoi HW, Yuen KY. In silico analysis of ORF1ab in coronavirus HKU1 genome reveals a unique putative cleavage site of coronavirus HKU1 3C-like protease. Microbiol Immunol 2005;49:899-908.
15. Xu X, Liu Y, Weiss S, Arnold E, Sarafianos SG, Ding J. Molecular model of SARS coronavirus polymerase: implications for biochemical functions and drug design. Nucleic Acids Res 2003;31:7117-30.
16. Hansen JL, Long AM, Schultz SC. Structure of the RNA-dependent RNA polymerase of poliovirus. Structure 1997;5:1109–22.
17. S. Doublie, T. Ellenberger, The mechanism of action of T7 DNA polymerase, Curr Opin Struct Biol 1998;8:704–712.
18. Elfiky AA. Anti-HCV, nucleotide inhibitors, repurposing against COVID-19. Life Sci 2020; 248:117477. doi: 10.1016/j.lfs.2020.117477.
19. Elfiky AA, Ismail AM. Molecular docking revealed the binding of nucleotide/side inhibitors to Zika viral polymerase solved structures. SAR QSAR Environ Res 2018; 29(5): 409-18. doi: 10.1080/1062936X.2018.1454981
20. Agostini ML, Andres EL, Sims AC, Graham RL, Sheahan TP, Lu X, Smith EC, Case JB, Feng JY, Jordan R, Ray AS, Cihlar T, Siegel D, Mackman RL, Clarke MO, Baric RS, Denison MR. Coronavirus Susceptibility to the Antiviral Remdesivir (GS-5734) Is Mediated by the Viral Polymerase and the Proofreading Exoribonuclease. mBio 2018;9(2):e00221-18. doi: 10.1128/mBio.00221-18.
21. Wang M, Cao R, Zhang L, Yang X, Liu J, Xu M, Shi Z, Hu Z, Zhong W, Xiao G. Remdesivir and chloroquine effectively inhibit the recently emerged novel coronavirus (2019-nCoV) *in vitro*. Cell Res 2020; 30(3):269-71. doi: 10.1038/s41422-020-0282-0
22. Kim UJ, Won EJ, Kee SJ, Jung SI, Jang HC. Combination therapy with lopinavir/ritonavir, ribavirin and interferon-α for Middle East respiratory syndrome. Antivir Ther 2016;21(5):455-9. doi: 10.3851/IMP3002.
23. Sheahan TP, Sims AC, Leist SR, Schäfer A, Won J, Brown AJ, Montgomery SA, Hogg A, Babusis D, Clarke MO, Spahn JE, Bauer L, Sellers S, Porter D, Feng JY, Cihlar T, Jordan R, Denison MR, Baric RS. Comparative therapeutic efficacy of remdesivir and combination lopinavir, ritonavir, and interferon beta against MERS-CoV. Nat Commun 2020;11(1):222. doi: 10.1038/s41467-019-13940-6.
24. Elfiky AA. SARS-CoV-2 RNA dependent RNA polymerase (RdRp) targeting: an *in-silico* perspective. J Biomol Struct Dyn 2021;39(9):3204-12. doi: 10.1080/07391102.2020.
25. Elfiky AA. Ribavirin, Remdesivir, Sofosbuvir, Galidesivir, and Tenofovir against SARS-CoV-2 RNA dependent RNA polymerase (RdRp): A molecular docking study. Life Sci 2020;253:117592. doi: 10.1016/j.lfs.2020.117592.
26. Nitulescu GM, Paunescu H, Moschos SA, Petrakis D, Nitulescu G, Ion GND, Spandidos DA, Nikolouzakis TK, Drakoulis N, Tsatsakis A. Comprehensive analysis of drugs to treat SARS-CoV-2 infection: Mechanistic insights into current COVID-19 therapies (Review). Int J Mol Med 2020;46(2):467-88. doi: 10.3892/ijmm.2020.4608
27. Keni R, Alexander A, Nayak PG, Mudgal J, Nandakumar K. COVID-19: Emergence, Spread, Possible Treatments,

and Global Burden. Front Public Health 2020;8:216. doi: 10.3389/fpubh.2020.00216.

28. Aftab SO, Ghouri MZ, Masood MU, Haider Z, Khan Z, Ahmad A, Munawar N. Analysis of SARS-CoV-2 RNA-dependent RNA polymerase as a potential therapeutic drug target using a computational approach. J Transl Med 2020;18(1):275. doi: 10.1186/s12967-020-02439-0.
29. Schwede T, Kopp J, Guex N, Peitsch MC. SWISS-MODEL: An automated protein homology-modeling server. Nucleic Acids Res 2003;31(13):3381-5. doi: 10.1093/nar/gkg520.
30. Messaoudi A, Belguith H, Ben Hamida J. Homology modeling and virtual screening approaches to identify potent inhibitors of VEB-1 β-lactamase. Theor Biol Med Model 2013;10:22. doi: 10.1186/1742-4682-10-22.
31. Laskowski RA, MacArthur MW, Moss DS, Thornton JM. PROCHECK a program to check the stereochemical quality of protein structures. J Appl Crystallogr 1993;26:283-91. doi: 10.1107/S0021889892009944.
32. Bowie JU, Lüthy R, Eisenberg D. A method to identify protein sequences that fold into a known three-dimensional structure. Science 1991; 253:164-70. doi: 10.1126/science.1853201.
33. Colovos C, Yeates TO. Verification of protein structures: patterns of nonbonded atomic interactions. Protein Sci. 1993;2:1511-19. doi: 10.1002/pro.5560020916.
34. Williams CJ, Headd JJ, Moriarty NW, Prisant MG, Videau LL, Deis LN, Verma V, Keedy DA, Hintze BJ, Chen VB, Jain S, Lewis SM, Arendall WB 3rd, Snoeyink J, Adams PD, Lovell SC, Richardson JS, Richardson DC. MolProbity: More and better reference data for improved all-atom structure validation. Protein Sci 2018;27(1):293-315. doi: 10.1002/pro.3330.
35. Chen VB, Arendall WB 3rd, Headd JJ, Keedy DA, Immormino RM, Kapral GJ, Murray LW, Richardson JS, Richardson DC. MolProbity: all-atom structure validation for macromolecular crystallography. Acta Crystallogr D Biol Crystallogr 2010;66(Pt-1):12-21. doi: 10.1107/S0907444909042073.
36. Wiederstein M, Sippl MJ. ProSA-web: interactive web service for the recognition of errors in three-dimensional structures of proteins. Nucleic Acids Res 2007;35: W407-10. doi: 10.1093/nar/gkm290.
37. Murail S, de Vries SJ, Rey J, Moroy G, Tufféry P. SeamDock: An Interactive and Collaborative Online Docking Resource to Assist Small Compound Molecular Docking. Front Mol Biosci 2021;8:716466. doi: 10.3389/fmolb.2021.
38. Altschul SF, Madden TL, Schäffer AA, Zhang J, Zhang Z, Miller W, Lipman DJ. Gapped BLAST and PSI-BLAST: a new generation of protein database search programs. Nucleic Acids Res 1997; 25(17):3389-402. doi: 10.1093/nar/25.17.3389.
39. Croll TI, Williams CJ, Chen VB, Richardson DC, Richardson JS. Improving SARS-CoV-2 structures: Peer review by early coordinate release. Biophys J 2021;120(6):1085-96. doi: 10.1016/j.bpj.2020.12.029.
40. Rice DW, Eisenberg D. A 3D-1D substitution matrix for protein fold recognition that includes predicted secondary structure of the sequence. J Mol Biol 1997;267(4):1026-38. doi: 10.1006/jmbi.1997.0924.
41. Waghmare S, Buxi A, Nandurkar Y, Shelke A, Chavan R. In silico sequence analysis, homology modeling and function annotation of leishmanolysin from Leishmania donovani. J Parasit Dis 2016; 40(4):1266-9. doi: 10.1007/s12639-015-0665-1.
42. Davis IW, Murray LW, Richardson JS, Richardson DC. MOLPROBITY: structure validation and all-atom contact analysis for nucleic acids and their complexes. Nucleic Acids Res 2004;32: W615-9. doi: 10.1093/nar/gkh398.
43. Studer G, Rempfer C, Waterhouse AM, Gumienny R, Haas J, Schwede T. QMEANDisCo-distance constraints applied on model quality estimation. Bioinformatics 2020; 36(6):1765-71. doi: 10.1093/bioinformatics/btz828.
44. Khater I, Nassar A. Potential antiviral peptides targeting the SARS-CoV-2 spike protein. BMC Pharmacol Toxicol 2022;23(1):91. doi: 10.1186/s40360-022-00627-w